Monthly Notices
of the
ROYAL ASTRONOMICAL SOCIETY

MNRAS **447,** 3029–3033 (2015) doi:10.1093/mnras/stu2653

The hard X-ray spectrum of NGC 5506 as seen by *NuSTAR*

G. Matt,[1⋆] M. Baloković,[2] A. Marinucci,[1] D. R. Ballantyne,[3] S. E. Boggs,[4] F. E. Christensen,[5] A. Comastri,[6] W. W. Craig,[5,7] P. Gandhi,[8,9] C. J. Hailey,[10] F. A. Harrison,[2] G. Madejski,[11] K. K. Madsen,[2] D. Stern[12] and W. W. Zhang[13]

[1]*Dipartimento di Matematica e Fisica, Università degli Studi Roma Tre, via della Vasca Navale 84, I-00146 Roma, Italy*
[2]*Cahill Center for Astronomy and Astrophysics, California Institute of Technology, Pasadena, CA 91125, USA*
[3]*Center for Relativistic Astrophysics, School of Physics, Georgia Institute of Technology, Atlanta, GA 30332, USA*
[4]*Space Sciences Laboratory, University of California, Berkeley, CA 94720, USA*
[5]*DTU Space National Space Institute, Technical University of Denmark, Elektrovej 327, DK-2800 Lyngby, Denmark*
[6]*INAF Osservatorio Astronomico di Bologna, via Ranzani 1, I-40127 Bologna, Italy*
[7]*Lawrence Livermore National Laboratory, Livermore, CA 94550, USA*
[8]*Department of Physics, University of Durham, South Road, Durham DH1 3LE, UK*
[9]*School of Physics and Astronomy, University of Southampton, Highfield, Southampton SO17 1BJ, UK*
[10]*Columbia Astrophysics Laboratory, Columbia University, New York, NY 10027, USA*
[11]*Kavli Institute for Particle Astrophysics and Cosmology, SLAC National Accelerator Laboratory, Menlo Park, CA 94025, USA*
[12]*Jet Propulsion Laboratory, California Institute of Technology, Pasadena, CA 91109, USA*
[13]*NASA Goddard Space Flight Center, Greenbelt, MD 20771, USA*

Accepted 2014 December 12. Received 2014 November 25; in original form 2014 October 8

ABSTRACT

NuSTAR observed the bright Compton-thin, narrow-line Seyfert 1 galaxy, NGC 5506, for about 56 ks. In agreement with past observations, the spectrum is well fitted by a power law with $\Gamma \sim 1.9$, a distant reflection component and narrow ionized iron lines. A relativistically blurred reflection component is not required by the data. When an exponential high-energy cutoff is added to the power law, a value of 720^{+130}_{-190} keV (90 per cent confidence level) is found. Even allowing for systematic uncertainties, we find a 3σ lower limit to the high-energy cutoff of 350 keV, the highest lower limit to the cutoff energy found so far in an AGN by *NuSTAR*.

Key words: accretion, accretion discs – galaxies: active – galaxies: individual: NGC 5506.

1 INTRODUCTION

Thanks to its grazing incidence optics, *NuSTAR* (Harrison et al. 2013) is providing, for the first time, source-dominated hard X-ray (>10 keV) observations of active galactic nuclei (AGN). The hard X-ray spectra can thus be studied in much greater detail than before, and spectral parameters determined with unprecedented precision and robustness.

The intrinsic X-ray spectra of (radio-quiet) AGN is believed to be produced by Comptonization of the accretion disc photons in a hot corona, with coronal temperatures well in excess of 10 keV (e.g. Perola et al. 2002; Malizia et al. 2014). One of the main goals of the *NuSTAR* AGN programme is to determine the coronal parameters (temperature, optical depth, location, geometry) and, at the very least, the exponential high-energy cutoff which, together with the power-law index, encodes information about these parameters.

Precise measurements of the high-energy cutoff (Baloković et al. 2015; Ballantyne et al. 2014; Brenneman et al. 2014a,b; Marinucci et al. 2014), or interesting lower limits to it (Marinucci et al. 2015; Matt et al. 2014) have already been obtained by *NuSTAR* for several AGN. In this paper we study the high-energy spectrum of the bright, nearby ($z = 0.006\,181$) Compton-thin (Wang et al. 1999) narrow-line Seyfert 1 Galaxy (Nagar et al. 2002), NGC 5506.

NGC 5506 has been observed by all major X-ray satellites. In the first *XMM–Newton* observation, clear evidence of narrow, neutral, and ionized iron lines were found (Matt et. al 2001; Bianchi & Matt 2002; Bianchi et al. 2003), but no evidence has been found of a broad component. One was later found by Guainazzi et al. (2010), albeit rather weak, when analysing all eight *XMM–Newton* observations obtained between 2001 February and 2009 January (see also Patrick et al. 2012 for *Suzaku* results). Simultaneous *XMM–Newton* and *BeppoSAX* observations permitted the search for a high-energy cutoff, which was found to be at 140^{+40}_{-30} keV, but with large systematic uncertainties due to ambiguities in the modelling (Bianchi et al. 2003, 2004).

This paper is structured as follows: Section 2 describes the observation and data reduction; Section 3 presents the spectral analysis, while the results are discussed in Section 4.

2 OBSERVATIONS AND DATA REDUCTION

NGC 5506 was observed with *NuSTAR* (OBSID 60061323) on 2014 April 1, as part of a snapshot survey of AGN selected from

⋆ E-mail: matt@fis.uniroma3.it

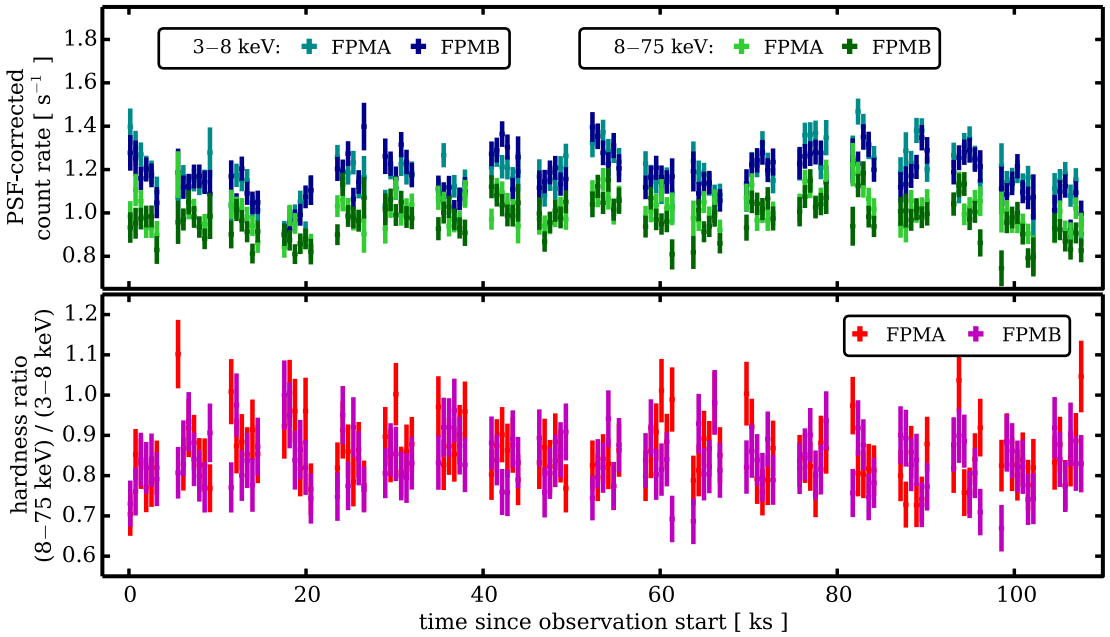

Figure 1. Upper panel: FPMA and FPMB light curves in the 3–8 keV and 8–75 keV energy ranges. Bins of 600 s are used. Lower panel: the (8–75 keV)/(3–8 keV) ratio.

the *Swift*/BAT all-sky survey (e.g. Baumgartner et al. 2013). The observation was coordinated with the *Swift* observatory (OBSID 00080413001), which observed the same target starting just 12 h later, on 2012 April 2. The *NuSTAR* and *Swift* observations are sufficiently close in time that they can be considered simultaneous as there is no evidence for spectral variability on this time-scale (see Fig. 1). The combined data therefore provide an instantaneous broad-band snapshot of the X-ray spectrum of NGC 5506 in the 0.8–80 keV band. The total *NuSTAR* and *Swift*/XRT exposures are 56 ks and 2.6 ks, respectively.

The *NuSTAR* data were reduced in the standard manner described in detail in Perri et al. (2013). We used HEASOFT v 6.15.1, NUSTARDAS v 1.3.1, and CALDB version 20131223. Following the event filtering using the `nupipeline` script, we extracted the source spectrum from a circular aperture 80 arcsec in radius centred on the peak of the point source image. The background extraction region covered the free area of the same detector, excluding the $\simeq$110 arcsec region around the source in order to avoid flux in the point spread function wings. The spectrum and the corresponding response files were generated using the `nuproducts` script. We bin the spectra for modules FPMA and FPMB to a minimum of 20 counts per bin before background subtraction, and fit them simultaneously, without co-adding. The cross-normalization constant is left free to vary in all our fits (with the instrumental normalization of FPMA fixed at unity).

We used online resources provided by the ASI Science Data Center (ASDC) for *Swift*/XRT data reduction,[1] HEASOFT v 6.13 and CALDB version 130313 were used for processing. The spectrum was extracted from a region with a radius of 20 arcsec centred on the brightest peak of emission, and the background was sampled from an annular region extending between 40 and 80 arcsec around the source. For spectral fitting we use the source spectrum binned to a minimum of 20 counts per bin before background subtraction. The cross-normalization constant is left free to vary in all our fits. We find it to be consistent with the expected systematic uncertainty of $\simeq$ 10 per cent determined from cross-calibration between *NuSTAR* and *Swift*/XRT (Madsen et al., in preparation).

3 SPECTRAL ANALYSIS

The analysis of the *NuSTAR* light curves shows the presence of flux variability of the order of 20 per cent, but without any significant spectral variability (Fig. 1). A hint of a hardening of the spectrum at lower fluxes is apparent, but it is easily explained by a small contribution from reflection from distant matter. Therefore, we used the spectra integrated over the entire observation. In all spectral fitting we combined the *NuSTAR* and *Swift*/XRT spectra, and included Galactic absorption with a column density of 3.8×10^{20} cm^{-2}.

All spectral fitting was done using the public package XSPEC. The reader is referred to its web page[2] for information on the fitting code and for details on the various spectral models applied here. Unless otherwise stated, all quoted errors correspond to 90 per cent confidence levels for one interesting parameter.

First, we fitted the spectra with a simple, absorbed power law with an exponential high-energy cutoff (CUTOFFPL model in XSPEC). The fit is unacceptable (χ^2/d.o.f. = 1989/1090), mostly due to a prominent iron line and curvature at high energies (see Fig. 2). As both features are suggestive of reflection, we added an XILLVER component (Garcia et al., 2013; actually the XILLVER-A-EC2 version, which includes both the angular dependence of the emitted radiation and a primary power law with an exponential cutoff[3]). This results in a dramatic improvement in the quality of the fit (χ^2/d.o.f. = 1150/1085). Further improvements are found by adding a MEKAL component (absorbed only by Galactic material) to account for some residuals in the soft X-ray band, which are likely due to the extended emission found by *Chandra* (Bianchi et al. 2003), and which result

[1] http://www.asdc.asi.it/mmia/

[2] http://heasarc.gsfc.nasa.gov/docs/xanadu/xspec/

[3] http://hea-www.cfa.harvard.edu/~javier/xillver/

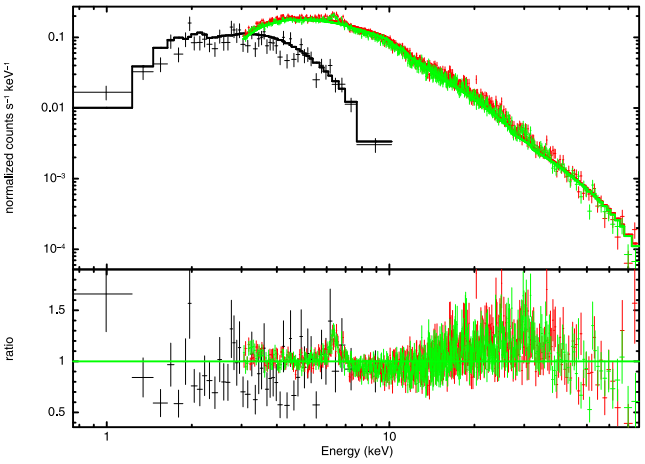

Figure 2. Spectra, best-fitting model, and data/model ratio when fitting with an absorbed, cutoff power law. Black refers to *Swift*/XRT data, red to *NuSTAR* FPMA and green to *NuSTAR* FPMB. The background is also plotted, showing that the source is larger than the background in the whole band.

Table 1. Best-fitting parameters for the model composed by an absorbed, cutoff power law, a reflection component and ionized iron lines. See text for details.

$N_{\rm H}$ (10^{22} cm^{-2})	$3.10^{+0.21}_{-0.20}$
Γ	1.91 ± 0.03
E_c (keV)	720^{+130}_{-190}
ξ (erg cm s^{-1})	22^{+15}_{-7}
A_{Fe}	1.63 ± 0.58
i	$<44^{\circ}$
$I_{\rm Fe\,XXV}$ (ph cm^{-2} s^{-1})	$<14.1 \times 10^{-6}$
$I_{\rm Fe\,XXVI}$ (ph cm^{-2} s^{-1})	$8.4(\pm6.4) \times 10^{-6}$

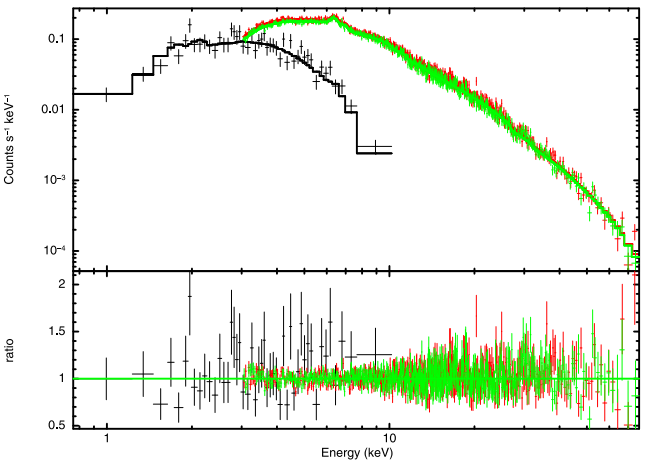

Figure 3. Spectra, best-fitting model and data/model ratio for the model composed of an absorbed, cutoff power law, a reflection component and ionized iron lines (see Table 1). Colours as in Fig. 2.

in χ^2/d.o.f. = 1144/1083; and adding Fe XXV and Fe XXVI narrow lines, following Matt et al. (2001) (χ^2/d.o.f. = 1135/1081). The best-fitting parameters are listed in Table 1, while the spectra, best-fitting model and data/model ratio are shown in Fig. 3. The various

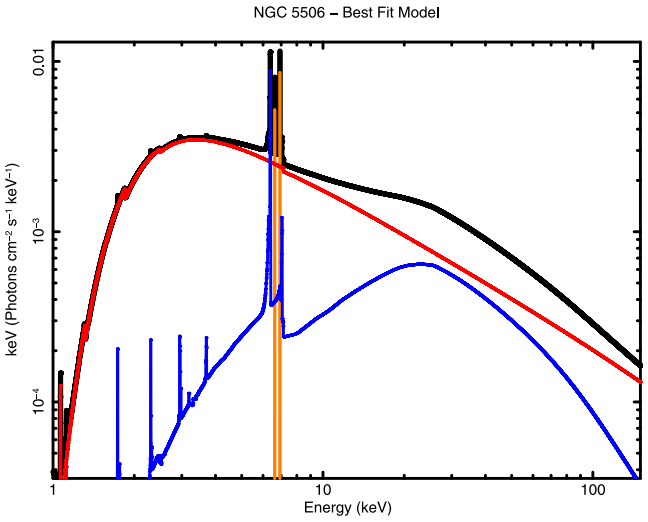

Figure 4. Best-fitting model for the model composed of: an absorbed cutoff power law (in red), a reflection component (in blue), ionized iron lines (in orange). The top black line is the total spectrum.

spectral components are shown in Fig. 4. The normalization of the reflection component corresponds to a standard R parameter (defined as the solid angle of the reflecting matter in units of 2π) of about 0.7. The observed 2–10 keV flux is 4.87×10^{-11} erg cm^{-2} s^{-1}; when corrected for absorption, the flux is 6.23×10^{-11} erg cm^{-2} s^{-1} corresponding to a luminosity of 5.26×10^{42} erg s^{-1}. This flux is at the lower end of the range of fluxes found so far for this source (Guainazzi et al. 2010).

Undoubtedly, the most interesting result relates to the high-energy cutoff. Figs 5 and 6, which show the correlation between the high-energy cutoff versus the power-law index and the normalization of the reflection component, respectively, indicate that the cutoff is very high (best-fitting value around 700 keV). Even with this very large value, the high-energy cutoff is constrained on both its lower and upper ends at the 3σ level. This shows the amazing capability of *NuSTAR* to measure this parameter (at least for a bright source with a relatively simple spectrum like NGC 5506), even for energies much higher than the 79 keV upper limit to the *NuSTAR* energy range. Even allowing for some remaining systematic errors in the effective area, which may affect the upper bounds of the contours in Figs 5 and 6, and given the fact (see below) that the result is robust against different modelling of the continuum, we can affirm that the cutoff energy is, at the 99.97 per cent confidence level, higher than 350 keV (see the appendix for further details).

The reflection component appears to be moderately ionized. Indeed, forcing the reflecting matter to be neutral results in a fit which is worse at the 99.99 per cent confidence level, according to an F-test. The measurement of the cutoff energy, however, remains basically unchanged. The iron abundance is 1.6 times higher than (but almost consistent with) solar, while the inclination of the reflecting surface with respect to the line of sight is found to be less than 44°. In an obscured source, in which the inclination angle of the accretion disc and the broad-line region is supposed to be high, this may indicate that the surface of the reflecting matter (which in the fitting model is assumed to be a slab) is misaligned with the disc surface, as indeed expected if it has a toroidal geometry.

Regarding the iron lines, we note that the flux of the neutral component (if fitted separately from the reflection component) is $6.87(^{+0.71}_{-1.05}) \times 10^{-5}$ ph cm^{-2} s^{-1}, consistent with most *XMM–Newton*

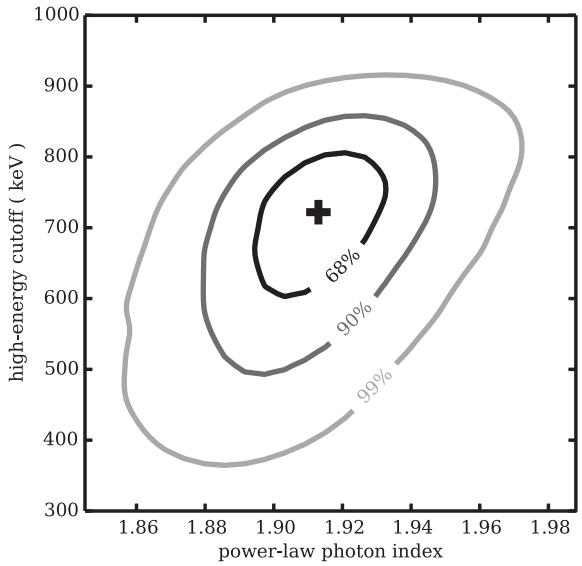

Figure 5. Power-law photon index and high-energy cutoff contour plot, calculated for the model composed of an absorbed, cutoff power law, a reflection component and ionized iron lines.

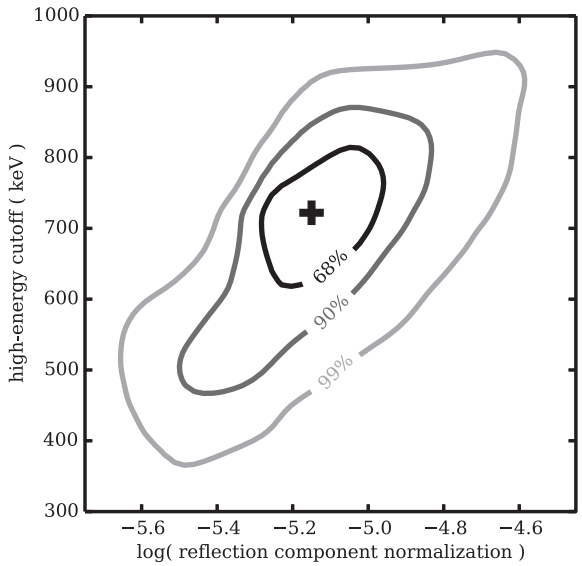

Figure 6. Normalization of the reflection component and high-energy cutoff contour plot, calculated for the model composed of an absorbed, cutoff power law, a reflection component and ionized iron lines.

observations but somewhat larger than the last two ones (Guainazzi et al. 2010). The fluxes of the He- and H-like lines are also consistent with most *XMM–Newton* observations, but a bit lower in case of two observations (Guainazzi et al. 2010). They are consistent with Suzaku measurements (Patrick et al. 2012).

Guainazzi et al. (2010) suggested the presence of a weak, broad component of the iron line. Therefore, we added an XILLVER-A-EC2 component blurred by relativistic effects (KDBLUR model). The χ^2/d.o.f. = 1127/1076 tells us that this component is required only at the 82 per cent confidence level, according to an F-test. That the reflection is mostly due to distant matter is corroborated by the fact that the flux of the neutral iron line (when fitted separately with a narrow Gaussian) is consistent with the values found in past observations, despite the large variations in the flux of the continuum. Not surprisingly, given the weakness of the relativistically blurred reflection the system parameters (among them the black hole spin) are unconstrained, and all other parameters – including the high-energy cutoff – remain basically unchanged.

Finally, assuming as customary that the primary power-law spectrum is due to Comptonization of thermal disc photons by hot electrons in a corona, we tried to estimate the coronal parameters by substituting the cutoff power law with a Comptonization model, namely COMPTT. For simplicity, the parameters of the reflection component, apart from the normalization, were kept frozen to the best-fitting values found with the cutoff power law. A slab geometry and seed photon temperature of 20 eV have been adopted. The fit is good (χ^2/d.o.f. = 1135/1084). The optical depth is found to be $0.02^{+0.19}_{-0.01}$, and the coronal electron temperature 440^{+230}_{-250} keV (consistent, within the errors, to the standard 2–3 factor between temperature and cutoff energy). Similar results are obtained with a spherical geometry, apart from a larger optical depth (about 0.09), as expected (in the spherical geometry the optical depth is the radial, thence effective, one while in the slab geometry the vertical – thence lower than effective – optical depth is used). Using instead the COMPPS model, a temperature of about 270 keV and an optical depth of 0.06 (0.14) are found for the slab (sphere) geometry.

4 DISCUSSION

We report on a joint *NuSTAR* and *Swift* observations of the bright, obscured narrow-line Seyfert 1 galaxy NGC 5506. The hard X-ray spectrum is composed of an absorbed (column density of about 3×10^{22} cm^{-2}) power law (with $\Gamma \sim 1.9$) with an exponential high-energy cutoff, plus a moderately ionized reflection component, and ionized iron lines. The presence of relativistically blurred reflection is not required by the data.

The most interesting result is the measurement of the high-energy cutoff, which demonstrates the capability of *NuSTAR* to constrain this. The best-fitting value is 720^{+130}_{-190} keV (90 per cent confidence level for one interesting parameter). Even at the 3σ level, the cutoff value is formally bound on both sides (see Fig. 5). Even allowing for possible systematic errors, we can conservatively put a firm lower limit to the cutoff energy of about 350 keV at the 99.97 per cent confidence level.

This is the highest lower limit to the cutoff energy found so far in an AGN by *NuSTAR*, and it is definitely inconsistent with values found in other AGN studied by *NuSTAR*, e.g. in SWIFT J2127.4+5654 (108 ± 11 keV; Marinucci et al. 2014), MCG-5-23-16 (116 ± 6 keV; Baloković et al. 2015), IC 4329A (186 ± 14 keV; Brenneman et al. 2014b) and 3C 382 (214^{+147}_{-63} keV in one of the two *NuSTAR* pointings, Ballantyne et al. 2014). Other lower limits, like those found in Ark 120 (>190 keV; Matt et al. 2014), 3C382 (>190 keV in the other *NuSTAR* pointing) and in NGC 2110 (>210 keV; Marinucci et al. 2015), while interesting, are nevertheless lower than the one found here in NGC 5506.

The above results, which suggest that very high cutoff energies do exist but are not too common, are still in agreement with the predictions of X-ray background (XRB) synthesis models. Gilli, Comastri & Hasinger (2007) showed that even a mean value of 300 keV would already saturate the XRB at 100 keV. Therefore, sources like NGC 5506 should be the exception rather than the rule.

While the number of AGN with a precise and robust measurement of the high-energy cutoff is still too small to search for correlations with system parameters, we cannot help noting that this parameter is quite different in the two best studied narrow-line Seyfert 1 galaxies observed so far by *NuSTAR*, namely NGC 5506 and SWIFT

J2127.4+5654 (even if we must note that NGC 5506 has X-ray properties, like e.g. the power-law index and the variability pattern, more similar to broad than that to narrow-line Seyfert 1s). The black hole mass of NGC 5506 is unfortunately very poorly known, with estimates ranging from 5×10^6 to 10^8 solar masses (see Guainazzi et al. 2010 and references therein), and the Eddington ratio is correspondingly uncertain, ranging from 0.007 to 0.14 (assuming that the bolometric luminosity is 20 times the 2–10 keV one). If the low value (indicated by the black hole mass measurement based on the central velocity dispersion) is the correct one, the two strictest lower limits to the cutoff energy, NGC 5506 and NGC 2110, are both found in sources with relatively low accretion rates, perhaps indicating inefficient cooling of the corona due to the low UV/soft X-ray flux.

ACKNOWLEDGEMENTS

This work has made use of data from the *NuSTAR* mission, a project led by the California Institute of Technology, managed by the Jet Propulsion Laboratory, and funded by the National Aeronautics and Space Administration. We thank the *NuSTAR* Operations, Software and Calibration teams for support with the execution and analysis of these observations. This research has made use of the *NuSTAR* Data Analysis Software (NUSTARDAS) jointly developed by the ASI Science Data Center (ASDC, Italy) and the California Institute of Technology (USA). GM, AM and AC acknowledge financial support from Italian Space Agency under grant ASI/INAF I/037/12/0-011/13. GM and AM also acknowledge financial support from the European Union Seventh Framework Programme (FP7/2007-2013) under grant agreement no. 312789. MB acknowledges support from the Fulbright International Science and Technology Award.

REFERENCES

Ballantyne D. R. et al., 2014, ApJ, 794, 62
Baloković M. et al., 2015, ApJ, in press
Baumgartner W. H., Tueller J., Markwardt C. B., Skinner G. K., Barthelmy S., Mushotzky R. F., Evans P. A., Gehrels N., 2013, ApJS, 207, 19
Bianchi S., Matt G., 2002, A&A, 387, 76
Bianchi S., Balestra I., Matt G., Guainazzi M., Perola G. C., 2003, A&A, 402, 141
Bianchi S., Matt G., Balestra I., Guainazzi M., Perola G. C., 2004, A&A, 422, 65
Brenneman L. W. et al., 2014a, ApJ, 781, 83
Brenneman L. W. et al., 2014b, ApJ, 788, 61
Cash W., 1979, ApJ, 228, 939
Garcia J., Dauser T., Reynolds C. S., Kallman T. R., McClintock J. E., Wilms J., Eikmann W., 2013, ApJ, 768, 146
Gilli R., Comastri A., Hasinger G., 2007, A&A, 463, 79
Guainazzi M., Bianchi S., Matt G., Dadina M., Kaastra J., Malzac J., Risaliti G., 2010, MNRAS, 406, 2013
Harrison F. A. et al., 2013, ApJ, 770, 103
Malizia A., Molina M., Bassani L., Stephen J. B., Bazzano A., Ubertini P., Bird A. J., 2014, ApJ, 782, L25
Marinucci A. et al., 2014, MNRAS, 440, 2347
Marinucci A. et al., 2015, MNRAS, 447, 160
Matt G., Guainazzi M., Perola G. C., Fiore F., Nicastro F., Cappi M., Piro L., 2001, A&A, 377, L31
Matt G. et al., 2014, MNRAS, 439, 3016
Nagar N. M., Oliva E., Marconi A., Maiolino R., 2002, A&A, 391, L21
Patrick A. R., Reeves J. N., Porquet D., Markowitz A. G., Braito V., Lobban A. P., 2012, MNRAS, 426, 2522
Perola G. C., Matt G., Cappi M., Fiore F., Guainazzi M., Maraschi L., Petrucci P. O., Piro L., 2002, A&A, 389, 802
Perri M. et al., 2013, The NuSTAR Data Analysis Software Guide. Available at: http://heasarc.gsfc.nasa.gov/docs/nustar/analysis/NuSTARDAS_swguide_v1.3.pdf
Ross R. R., Fabian A. C., 2005, MNRAS, 358, 211
Wang T., Mihara T., Otani C., Matsuoka M., Awaki H., 1999, ApJ, 515, 567

APPENDIX A: HOW ROBUST IS THE CUTOFF ENERGY MEASUREMENT?

As the main result of this paper is the tight lower limit to the cutoff energy, we tested the robustness of the results by making a few changes in either the data reduction or in the spectral modelling.

We adopted different extraction regions (40, 60, 80, 100 and 120 arcsec) and different binnings (20 counts per bin, 50 counts per bin, 100 counts per bin, S/N>5), and fitted the data with all possible combinations. The best-fitting cutoff energy varies somewhat, but remains always higher than 400 keV (and in most cases higher than 450–500 keV) at the 90 per cent confidence level apart from the 40 arcsec aperture (and 20 counts per bin) where the lower limit is 350 keV, very likely due to the lower number of source counts. The use of the Cash statistics (Cash 1979) instead of χ^2 statistics also does not significantly affect the results.

Another test we made was to substitute the XILLVER with the REFLIONX (Ross & Fabian 2005) reflection model, in a version which allows the primary emission to be a power law with an exponential cutoff. The latter model has no angular dependence, being an average over the emission angle. The fit is worse (χ^2/d.o.f. = 1150/1082, to be compared with χ^2/d.o.f. = 1135/1081 which we found using XILLVER), and a cutoff energy of ∼300 keV is found, with similar values for the other parameters. In this case, however, the addition of a relativistically blurred component results in a more significant fit improvement (χ^2/d.o.f. = 1124/1077, significant at the 99.98 per cent confidence level according to the F-test), and the cutoff energy is >390 keV. The ionization parameter and iron abundance are consistent with those found with the XILLVER model, while the power-law index is somewhat steeper, ∼2. The best-fitting emissivity index, inner disc radius and inclination angle are $1.84^{+1.05}_{-0.14}$, <2.6 gravitational radii and $84 \pm 4^{\circ}$, respectively, while the outer disc radius has been kept fixed to 400 gravitational radii.)

Finally, we note that the relative accuracy of the *NuSTAR* effective area at 70 keV is about 5 per cent (Madsen et al., in preparation). This means that the error on the high-energy cutoff is likely dominated by statistical, rather than systematic, uncertainties. Indeed, adding a 5 per cent systematic uncertainties to all energy bins – clearly a gross overestimate – only slightly larger errors on E_c are found: the best-fitting value is, adopting the same model as in Table 1, 756^{+139}_{-233} keV at 90 per cent confidence level, and 756^{+232}_{-325} keV at 3σ.

This paper has been typeset from a TEX/LATEX file prepared by the author.